Journal of Chromatography, 256 (1983) 1–15
Elsevier Scientific Publishing Company, Amsterdam — Printed in The Netherlands

CHROM. 15,379

THERMAL CONDUCTIVITY DETECTOR: THEORY AND NUMERICAL MODEL

GREGORY WELLS* and RICHARD SIMON
Varian Instrument Group, Walnut Creek Division, Walnut Creek, CA 94598 (U.S.A.)
(Received August 16th, 1982)

SUMMARY

A numerical model of all significant heat loss terms for a thermal conductivity detector has been developed and found to be in good agreement with theory. The sensitivity for the constant current, voltage and mean temperature modes has been shown to be equivalent at low sample concentrations. The constant temperature mode has been shown to have a higher sensitivity by a factor of 7–10, but an analysis of noise sources implies that the detectivity and signal-to-noise ratio are, at best, the same. The factors affecting the linear response at high concentrations in the four modes of operation have been investigated. The increased heat loss due to conduction through the ends of the filament, at high sample concentrations, has been found to improve the linear response in the constant current and voltage modes.

INTRODUCTION

Thermal conductivity detectors have been used since the beginning of gas chromatography. Numerous papers have been published describing and comparing the various modes of operation: constant voltage, constant current[1–3], constant temperature[4] and constant mean temperature[5,6]. Most of the work has been focused in the low sample concentration range where the response is linear, and where heat loss mechanisms other than thermal conductivity are constant. In this work, the effects of conduction, radiation and mass transport on the response of a thermal conductivity detector operating in these various modes have been explored. In particular these effects in the high concentration range have been examined.

SENSITIVITY FOR CONSTANT VOLTAGE, CURRENT AND MEAN TEMPERATURE OPERATION

Consider a filament whose resistance at temperature $t = 0°C$ is R_0 and through which passes a current i. The heat balance equation is given by

$$i^2 R_0 (1 + \alpha t) = Q_{con} + Q_{cr} + Q_{mt} \quad (1)$$

0021-9673/83/0000-0000/$03.00

where

$Q_{con} = G\,\lambda(t - t_w)$;
α = temperature coefficient of resistance;
t = filament temperature;
t_w = wall temperature;
G = cell geometry factor;
λ = thermal conductivity of gas;
Q_{cr} = power loss due to conduction and radiation;
Q_{mt} = power loss due to mass transport.

The three terms on the right-hand side of eqn. 1 represent the heat loss due to (1) the thermal conductivity of the gas, (2) conduction and radiation and (3) mass transport.

If we initially restrict the discussion to the low concentration range where the change in filament temperature will be small, the terms Q_{cr} and Q_{mt} can be written as

$$Q_{cr} = k_1 (t - t_w) \tag{2}$$

$$Q_{mt} = k_2 (t - t_w) \tag{3}$$

Further justification for this form will be given later. Thus, the heat balance eqn. 1 becomes

$$i^2 R_0 (1 + \alpha t) = J (t - t_w) \tag{4}$$

where the effective conductivity J is

$$J = G\,\lambda + k_1 + k_2 \tag{5}$$

Eqn. 4 is the more familiar form that is usually encountered.

For the purpose of this discussion a four-filament bridge configuration, as shown in Fig. 1, is assumed, in which the sample (R_s) and reference (R_r) filament resistances are equal in the absence of a sample. Further, because of the symmetry of the bridge, the current flowing through any element will be the same, even in the presence of sample. This does not mean, however, that the current is necessarily constant. This type of bridge is generally used in the constant voltage, current or mean temperature mode. Let i, J_0 and t be the initial current, conductivity and filament temperature and let δi be the decrease in current due to a decrease in effective conductivity δJ. The quantities δi and δJ are small although not necessarily infinitesimal. Let δt_s and δt_r be the temperature change on the filaments. The power balance equations for the sample and reference filaments are as follows:

Sample:

$$(i - \delta i)^2 R_0[1 + \alpha(t + \delta t_s)] = (J_0 - \delta J)(t + \delta t_s - t_w) \tag{6}$$

Reference:

$$(i - \delta i)^2 R_0[1 + \alpha(t - \delta t_r)] = J_0 (t - \delta t_r - t_w) \tag{7}$$

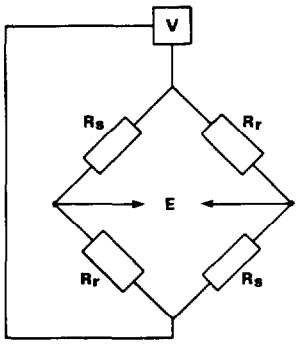

Fig. 1. Constant current and voltage bridge configuration.

Dividing eqn. 6 by eqn. 7, cross-multiplying and neglecting all terms of higher order than one, we obtain

$$(\delta t_r + \delta t_s)[-(1 + \alpha t)J_0 + \alpha J_0 (t - t_w)] = (1 + \alpha t)(-\delta J)(t - t_w) \quad (8)$$

or

$$(\delta t_r + \delta t_s) = \frac{\delta J}{J_0}(t - t_w)\frac{(1 + \alpha t)}{(1 + \alpha t_w)} \equiv H \quad (9)$$

The quantity H on the right-hand side of eqn. 9 is a system invariant for the constant voltage, current and mean temperature modes.

The choice of regulation mode imposes an additional constraint on eqns. 6 and 7, and determines the exact values of δt_s and δt_r. In the constant voltage (CV) mode a decrease in conductivity δJ causes an increase in the temperature (and resistance) of the sample filament by an amount δt_s. Because the voltage across the bridge is constant, the current through the sample and reference filament must, therefore, be reduced. This results in a decrease in the reference filament temperature by δt_r. The sum of these changes, $\delta t_s + \delta t_r$, is given in eqn. 9 by H. In the constant current (CC) mode no change occurs in the reference filament; thus $\delta t_r = 0$ and, therefore, $\delta t_s = H$. In the constant mean temperature (CM) mode the power applied to the bridge is varied as δJ changes in such a way that the equivalent resistance ("mean resistance") of the bridge remains constant. This implies that $\delta t_s = \delta t_r \equiv \delta t$. Thus $2\delta t = H$.

If the response is defined as the imbalance in the bridge E (Fig. 1), then in the constant current mode

$$E_{CC} = i(R_s - R_r) \quad (10a)$$

$$= iR_0\{[1 + \alpha(t + \delta t_s)] - (1 + \alpha t)\} \quad (10b)$$

$$= iR_0\alpha\delta t_s \quad (10c)$$

Using eqn. 9 and the fact that $\delta t_s = H$, the result is

$$E_{CC} = i\,R_0\alpha H \tag{10d}$$

For the constant voltage mode, assuming the same initial conditions and current, the response is

$$E_{CV} = (i - \delta i_{CV})\,(R_s - R_r) \tag{11a}$$

$$= (i - \delta i_{CV})\,R_0\,\{[1 + \alpha(t + \delta t_s)] - [1 + \alpha(t - \delta t_r)]\} \tag{11b}$$

$$= i\,R_0\,\alpha(\delta t_s + \delta t_r) - R_0\alpha\delta i_{CV}\,(\delta t_s + \delta t_r) \tag{11c}$$

where δi_{CV} is the decrease in bridge current due to the presence of sample. If the higher order terms in δ are neglected, the result is

$$E_{CV} = i\,R_0\alpha H \tag{11d}$$

Similarly, for the constant means temperature mode one obtains

$$E_{CM} = (i - \delta i_{CM})\,(R_s - R_r) \tag{12a}$$

$$= (i - \delta i_{CM})\,R_0\,\{[1 + \alpha(t + \delta t)] - [1 + \alpha(t - \delta t)]\} \tag{12b}$$

$$= iR_0\alpha 2\delta t - R_0\alpha 2\delta t\,\delta i_{CM} \tag{12c}$$

$$= i\,R_0\alpha H \tag{12d}$$

Thus, the sensitivity ($S = E/\delta J$) is equivalent for all three modes of operation, provided that the temperature and current changes remain small. The noise sources should also be the same. Therefore, the signal-to-noise ratio (and detectivity) must also be identical. The response can be expressed in alternative forms:

$$E = \frac{iR_0\dfrac{\delta J}{J_0}(1 + \alpha t)}{\dfrac{(1 + \alpha t)}{\alpha(t - t_w)} - 1} \tag{13a}$$

or

$$E = \left[iR_0\,\alpha\cdot\frac{\delta J}{J_0}\right](t - t_w)\left[\frac{1 + \alpha t}{1 + \alpha t_w}\right] \tag{13b}$$

The latter expression is similar to one derived by Wittebrood[4] and others[1–3], with the exception of the last term, which occurs because the usual approximation of $\delta t_r = 0$ was not used here. This correction term has a typical value of 1.1–1.2.

SENSITIVITY FOR CONSTANT TEMPERATURE OPERATION

The constant temperature mode of operation is shown in Fig. 2. The bridge generally consists of a single active filament R_s with a passive load resistance R_L on one side of the bridge with balance resistances R_1 and R_2 on the other side. The balance resistances are much larger than R_L or R_S and therefore draw negligible current from the power supply. The supply voltage V is decreased by δV in response to a decrease δJ in conductivity so that R_S remains constant. The power balance equation is again given by eqn. 4. Using the relationship

$$i = V/[R_L + R_0 (1 + \alpha t)] \tag{14}$$

yields

$$V^2 = \frac{(R_L + R_s)^2 J(t - t_w)}{R_L} \tag{15}$$

where

$$R_s = R_0 (1 + \alpha t) \tag{16}$$

For a small change δJ in eqn. 15, the corresponding change δV is

$$2V\delta V = \frac{\delta J (R_L + R_s)^2 (t - t_w)}{R_L} \tag{17a}$$

$$\delta V = \frac{i\delta J}{J} \cdot \frac{(R_L + R_s)}{2} \tag{17b}$$

As δJ is small, $J = J_0 - \delta J \approx J_0$, and

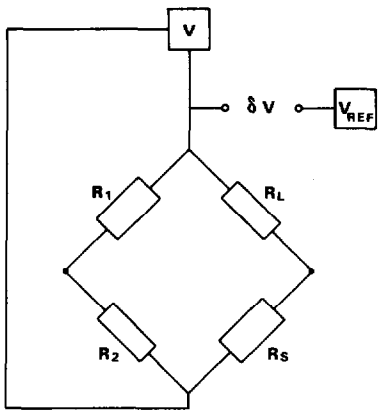

Fig. 2. Constant temperature bridge configuration.

$$\delta V = \frac{i\delta J}{J_0} \cdot \frac{(R_L + R_s)}{2} \tag{17c}$$

If $R_L = |R_s| = |R_0(1 + \alpha t)|$, then

$$\delta V = iR_0 \cdot \frac{\delta J}{J_0}(1 + \alpha t) \tag{18}$$

Comparison of eqn. 18 with eqn. 13a shows that the CT mode has higher sensitivity than the other three because the term in the denominator of eqn. 13a has values ranging from 7 to 10. This is not meant to imply, however, that the detectivity or signal-to-noise ratio is any better.

CONSTANT MEAN TEMPERATURE MODE --OUTER BRIDGE

The large disparity in sensitivity between the CT and CM modes is anomalous and exists in part because the response in the CT mode is taken to be the change in applied bridge voltage δV (Fig. 2); where as in the CM mode it is usually taken within the bridge E (Fig. 1). Consider an alternative method of measuring the response in the CM mode. Let the active filament R_s in Fig. 2 be replaced by the four-filament bridge of Fig. 1. This becomes the control circuit for the CM mode. However, instead of using E as a measure of the response let us use δV. This will be referred to as the outer bridge configuration. The change δV is given by:

$$\delta V = 2\delta i (R_L + R_B) \tag{19}$$

where R_B is the equivalent resistance of the four-filament sensing bridge. The factor 2 arises because δi as defined previously as the change in current on only one side of the bridge in Fig. 1. Eqns. 6 and 7 still apply with $\delta t_s = \delta t_r$. Using eqn. 7 the current change δi is found to be

$$\delta i = i - \left\{\frac{J_0(t - \delta t - t_w)}{R_0[1 + \alpha(t - \delta t)]}\right\}^{1/2} \tag{20}$$

Using eqn. 4 and letting $J = J_0$, as i is the current when $\delta J = 0$, we obtain

$$\delta i = \left[\frac{J_0(t - t_w)}{R_0(1 + \alpha t)}\right]^{1/2} - \left[\frac{J_0(t - \delta t - t_w)}{R_0(1 + \alpha t)}\right]^{1/2} \left\{\frac{R_0(1 + \alpha t)}{R_0[1 + \alpha(t - \delta t)]}\right\}^{1/2} \tag{21}$$

Rearranging terms yields

$$\delta i = \left[\frac{J_0(t - t_w)}{R_0(1 + \alpha t)}\right]^{1/2} \left\{1 - \left[1 - \frac{\delta t}{(t - t_w)}\right]^{1/2} \left[\frac{1}{1 - \frac{\alpha\delta t}{(1 + \alpha t)}}\right]^{1/2}\right\} \tag{22}$$

Expanding the square root terms and neglecting the higher order terms in δt results in

$$\delta i = \left[\frac{J_0 (t - t_w)}{R_0 (1 + \alpha t)}\right]^{1/2} \left\{1 - \left[1 - \frac{\delta t}{2(t - t_w)}\right] \left[1 + \frac{\alpha \delta t}{2(1 + \alpha t)}\right]\right\} \tag{23}$$

Neglecting the higher order terms in δt gives

$$\delta i = \left[\frac{J_0 (t - t_w)}{R_0 (1 + \alpha t)}\right]^{1/2} \left[\frac{1}{(t - t_w)} - \frac{\alpha}{(1 + \alpha t)}\right] \frac{\delta t}{2} \tag{24}$$

Therefore, eqn. 19 becomes

$$\delta V = 2i(R_L + R_B) \left[\frac{1}{(t - t_w)} - \frac{\alpha}{(1 + \alpha t)}\right] \frac{\delta t}{2} \tag{25}$$

As $\delta t = H/2$ from eqn. 9, then

$$\delta V = i \cdot \frac{\delta J}{J_0} \cdot \frac{(R_L + R_B)}{2} \left[\frac{1}{(t - t_w)} - \frac{\alpha}{(1 + \alpha t)}\right] \left[\frac{(t - t_w)}{1 - \dfrac{\alpha(t - t_w)}{(1 + \alpha t)}}\right] \tag{26a}$$

$$\delta V = \frac{i \delta J}{J_0} \cdot \frac{(R_L + R_B)}{2} \left[\frac{1}{1 - \dfrac{\alpha(t - t_w)}{(1 + \alpha t)}} - \frac{\alpha(t - t_w)}{(1 + \alpha t) - \alpha(t - t_w)}\right] \tag{26b}$$

$$\delta V = i \cdot \frac{\delta J}{J_0} \left[\frac{(R_L + R_B}{2}\right] \tag{26c}$$

Comparison with eqn. 17c shows that the CT mode has the same sensitivity as the CM mode when the response is measured at the same place in the bridge circuit. The noise sources for these two modes are not necessarily the same, even if the circuit elements are the same (*i.e.*, $R_B = R_S$, and the same amplifiers are used in the feedback control loop and signal output stages). Because of the higher bridge current in the CM mode, its noise will be greater than that in the CT mode, when measured in the outer bridge configuration.

COMPARISON OF SIGNAL-TO-NOISE RATIO

Although a comparison of the sensitivities in the various operating modes can be made without regard to the details of the electronics, the same cannot be done for the noise sources. However, some general statements can be made that allow an ordering of signal-to-noise ratios for the various modes.

In the CM, CV and CC modes, the bridge (Fig. 1) efficiently rejects power supply noise as it is common to both sides of the bridge and appears at both inputs to the signal amplifier (E, Fig. 1). The dominant noise at the output of the signal amplifier will consist of shot noise at the input stage and flow-induced temperature fluctuations of the sensing filaments. These same noise sources are present in the CT mode. In addition, the power supply requires a high gain feedback loop with a higher

bandwidth for stability of the constant temperature system, in order to respond fast enough to keep the temperature of the filament constant. This means that noise from the filament or any other part of the feedback loop will be amplified and will appear at one input to the signal amplifier (δV, Fig. 2). This noise will not be rejected since it is not common to both inputs to the signal amplifier. Also noise from the reference supply (Fig. 2) likewise is not rejected because it appears at only one input. Therefore, even if the measurement bandwidth is the same, the noise equivalent bandwidth for the CT mode will be significantly larger. Generally the signal-to-noise ratio for the CT mode is less than the CM, CV or CC modes.

LINEAR RANGE

At low sample concentrations all four modes provide a linear response due to the direct proportionality between $\delta J/J_0$ and the molar fraction of the sample, X, which has been shown by Lindsay and Bromley[7] to be

$$\frac{\delta J}{J_0} \approx X\left(A - \frac{\lambda_1}{\lambda_2 B}\right) \tag{27}$$

where

λ_1 = conductivity of carrier gas;
λ_2 = conductivity of sample;
A, B = constants.

At higher concentrations not only does eqn. 27 fail, but so do the approximations that were made in eqns. 2, 3 and 4. When the change in filament temperature is no longer negligible, then the alternative heat loss terms Q_{mt} and Q_{cr} must be considered. Under these circumstances an explicit form for the response cannot be found. Therefore, a numerical model based on eqn. 1 was developed and used to determine the response in different modes of operation.

Explicit functional forms for Q_{mt} and Q_{cr} were found by experimentally measuring these quantities independently and fitting them to a function. The heat loss by conduction and radiation was determined by measuring the power into the bridge as a function of filament temperature, in an evacuated cell. These data were then least square fit to an equation of the form

$$Q_{cr} = B_{cr}\,\Delta t \qquad 0 \leqslant \Delta t \leqslant t_{max} \tag{28a}$$

$$Q_{cr} = A_{cr} + B'_{cr}\,\Delta t + C_{cr}\,\Delta t^2 \qquad t_{max} < \Delta t \tag{28b}$$

where $\Delta t = t - t_w$. For small changes in Δt only eqn. 28a is important, which is of the form of eqn. 2, where $k_1 = B_{cr}$. This form was chosen because $\lim_{t \to t_w} Q_{cr} = 0$. The quadratic term when $t > t_{max}$ is due to radiation losses, whereas the linear terms are due to conduction through the ends of the filaments. The additional constraint that the slopes of Q_{cr} at t_{max} are the same was imposed to make Q_{cr} a smooth function.

The specific form for Q_{mt} was taken to be:

$$Q_{mt} = F \int_{t_w}^{t_0} C_p(t, X)\mathrm{d}t \tag{29}$$

where

F = molar flow-rate at t_w;
C_p = heat capacity of the gas mixture;
t_0 = temperature of gas leaving cell.

The heat capacity of the mixture was approximated by

$$C_p = C_{p1}(1 - X) + C_{p2}X \tag{30}$$

where

C_{p1} = heat capacity of carrier gas as a function of temperature;
C_{p2} = heat capacity of sample as a function of temperature.

The temperature of the gas leaving the cell was approximated by

$$t_0 = t_w + A\,t + B\,t^2 \tag{31}$$

where

$$A = A_0 + A_1X + A_2X^2 \tag{32a}$$

$$B = B_0 + B_1X + B_2x^2 \tag{32b}$$

and X is the molar fraction of sample. As $t_0 \approx t_w$, eqn. 29 can be replaced by

$$Q_{mt} = F(A\Delta t + B\Delta t^2)C_p \tag{33}$$

For small changes in F and Δt the quadratic term can be neglected and eqn. 33 reduces to eqn. 3 with $k_2 = FAC_p$.

As the amount of heat transferred to the gas is a complicated function of flow dynamics and cell geometry, the data used to find the constants in eqn. 32 were obtained by measuring the bridge imbalance as a function of flow, when a constant concentration of sample flowed through all four elements of the bridge. This was done for different concentrations of sample and for several filament temperatures.

The geometric factor in eqn. 1 was taken to be

$$G = \frac{2\pi L}{\ln(r_w/r_f)} \tag{34}$$

where

L = length of filament
r_w = radius of cell wall
r_f = radius of filament

TABLE I

CONSTANTS USED IN CALCULATIONS

$B_{cr} = 1.006 \cdot 10^{-3}$ J/°C	$\alpha = 3.3 \cdot 10^{-3}$ ohm/°C
$A_{cr} = 4.332 \cdot 10^{-6}$ J	$R_0 = 29.41$ ohm
$B'_{cr} = 9.973 \cdot 10^{-4}$ J/°C	$L = 13.8$ mm
$C_{cr} = 2.166 \cdot 10^{-7}$ J/(°C)^2	$r_w = 1.27$ mm
$t_{max} = 20$°C	$r_f = 0.23$ mm
$C_{p1} = 4.96$ cal/°C	$\lambda_1 = 422.08 \cdot 10^{-6}$ cal/(sec)(cm^2)(°C/cm)
$C_{p2} = 13.22$ cal/°C	$\lambda_2 = 60.55 \cdot 10^{-6}$ cal/(sec)(cm^2)(°C/cm)
$A_0 = 2.079 \cdot 10^{-3}$	$A = 4.0$
$A_1 = 1.357 \cdot 10^{-2}$	$B = 0.6$
$A_2 = 2.721 \cdot 10^{-7}$	$C_{11} = 341.1 \cdot 10^{-6}$ cal/(sec)(cm^2)(°C/cm)
$B_0 = 3.938 \cdot 10^{-5}$	$C_{21} = -7.674 \cdot 10^{-5}$ °K
$B_1 = 1.045 \cdot 10^{-4}$	$C_{12} = 57.2 \cdot 10^{-6}$ cal/(sec)(cm^2)(°C/cm)
$B_2 = 5.139 \cdot 10^{-6}$	$C_{22} = -2.213 \cdot 10^{-5}$ °K

The conductivity term was fitted to the equation given by Chapman and Cowling[8]:

$$\lambda = \frac{\lambda_1}{1 + A(X/1 - X)} + \frac{\lambda_2}{1 + B((1 - X)/X)} \tag{35}$$

The constants A and B were determined from the response of the bridge operated in the CM mode, where it was assumed that an increase in the filament temperature did not cause a significant change in Q_{mt} and Q_{cr}. This is a valid approximation as the constants A and B were found to be only weak functions of temperature. The temperature dependence of λ_1 and λ_2 followed the form given by Benson[9] for gas viscosity:

$$\lambda(T)_i = \frac{C_{1i}}{1 + C_{2i}/T} \tag{36}$$

(100°K $< T <$ 800°K), where C_1 and C_2 are constants.

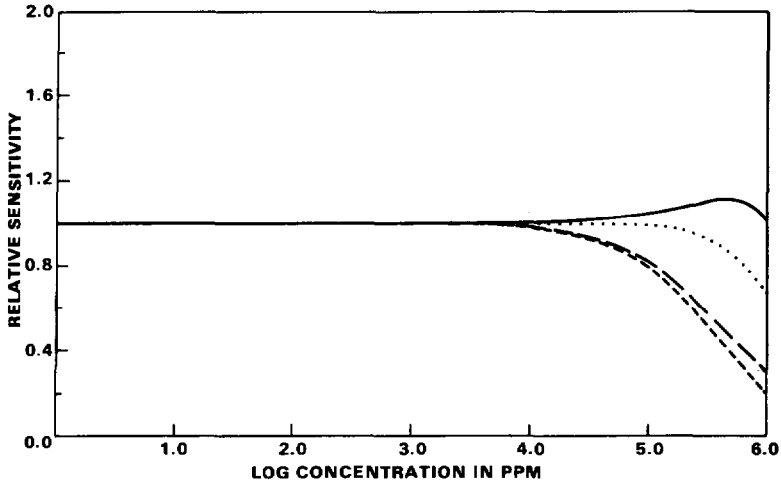

Fig. 3. Relative sensitivity *versus* concentration for butane in helium. (---) Constant temperature; - - -, constant mean temperature; · · · · ·, constant voltage; ——, constant current.

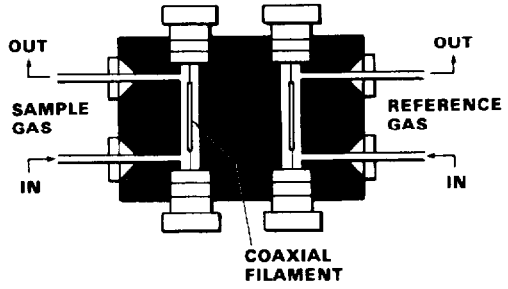

Fig. 4. Thermal conductivity cell.

RESULTS OF MODEL

The model developed here allows the independent choice of t_w, L, r_w, r_f and R_0 for each of the four filaments, as well as different flows for the sample and reference sides of the bridge. Using the constants described in the previous section that were determined for butane in helium as carrier gas, the sensitivities in the four modes were calculated. Here the sensitivity is defined to be $S \equiv E/C$, where C is the sample concentration. The constants used in the calculations are listed in Table I. The results are shown in Fig. 3 for an initial temperature $t = 170°C$ and $t_w = 120°C$. These are calculated results and were found to agree with the measured data to within a few percent across the entire concentration range. Currents from 80 to 150 mA (160–300 mA total bridge current) were investigated. The relative sensitivities for the different modes were found to be unchanged throughout the range of currents, except for the CC mode, which showed a slight shift in the maximum towards lower concentration at higher currents. The cell (Fig. 4) used for these studies was a Varian 3700 thermal conductivity detector[5]. It can be seen that the CV mode provides significantly better linearity than either the CT, CC or CM modes. It is interesting that there is no

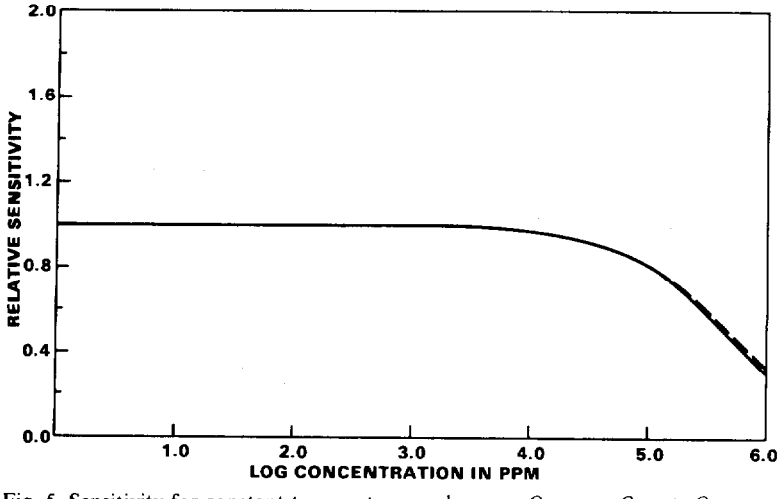

Fig. 5. Sensitivity for constant temperature mode. ---, Q_{con}; ···, $Q_{con} + Q_{cr}$; ——, $Q_{con} + Q_{cr} + Q_{mt}$.

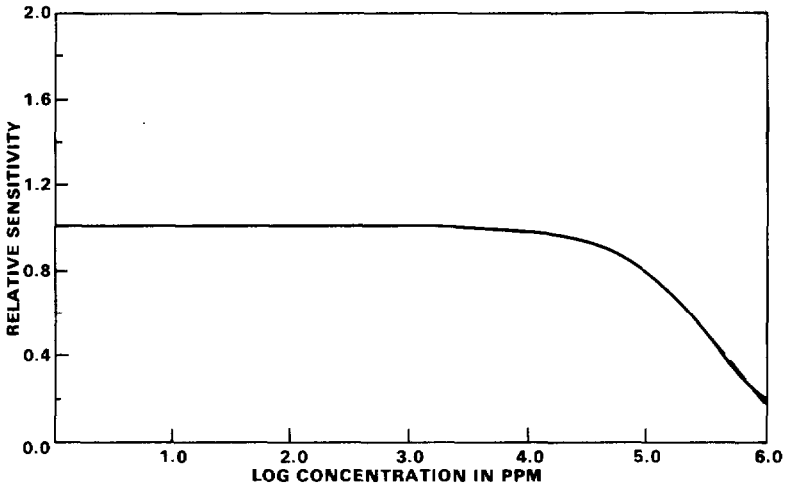

Fig. 6. Sensitivity for constant mean temperature mode. – – –, Q_{con}; · · ·, $Q_{con} + Q_{cr}$; ——, $Q_{con} + Q_{cr} + Q_{mt}$.

positive curvature in either the CT or CV modes as was predicted by Wittebrood[4], who neglected the change in Q_{mt} and Q_{cr} that occurs at high sample concentrations.

The advantage of the numerical model is that the importance of each heat loss mechanism may be independently observed. Figs. 5–8 show calculated sensitivities for the different modes of operation. In each calculation the effect of including the different heat loss terms Q_{con}, Q_{cr} and Q_{mt} can be seen. The heat loss by mass transport is relatively unimportant in affecting the sensitivity at high concentrations, in all modes. The effect of heat loss by conduction and radiation (primarily conduction), however, significantly changes the sensitivity at higher concentrations for the CV and CC modes. The importance of this effect is most dramatic in the CV mode (Fig. 7) where

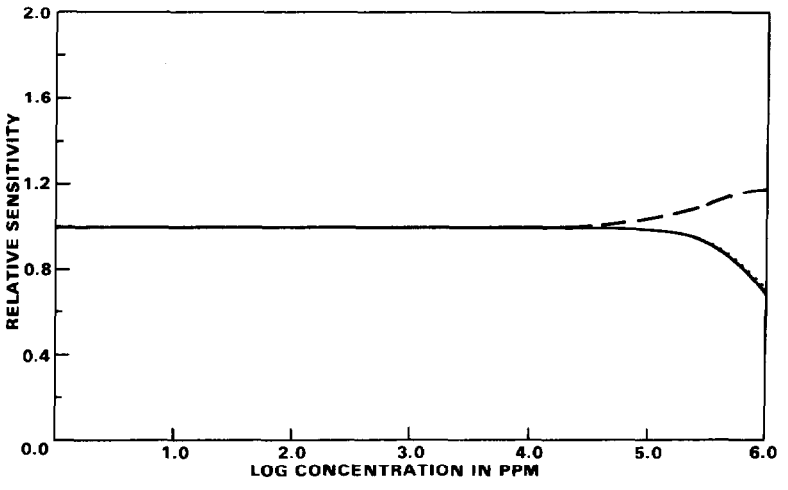

Fig. 7. Sensitivity for constant voltage mode. – – –, Q_{con}; · · ·, $Q_{con} + Q_{cr}$; ——, $Q_{con} + Q_{cr} + Q_{mt}$.

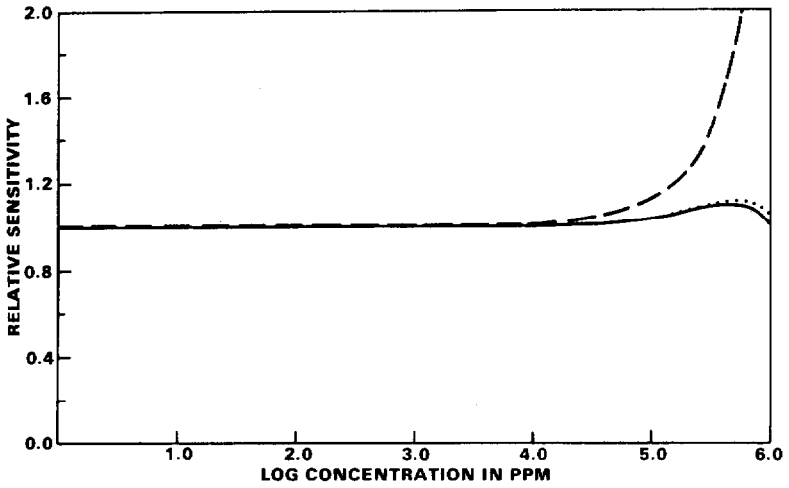

Fig. 8. Sensitivity for constant current mode. ---, Q_{con}; ···, $Q_{con} + Q_{cr}$; — -, $Q_{con} + Q_{cr} + Q_{mt}$.

the sensitivity curves up when Q_{cr} is not included and curves down when it is. This implies that by optimizing the heat loss Q_{cr} the linear range can be extended.

The change in linear response at concentrations beyond 1% is the result of increases in the sample filament temperatures (Fig. 9) and decreases in the bridge current (Fig. 10). The differences between the various modes of operation are due to the different magnitudes of changes in filament temperature and current. These differences are the result of the variation in the power into the filaments and the change in the distribution of power dissipation between Q_{con} and Q_{cr}. For example, the power into the sample filament in the CM mode decreases at higher concentrations (Fig. 11), while the dissipation by Q_{cr} remains almost unchanged. In the CV mode however, the

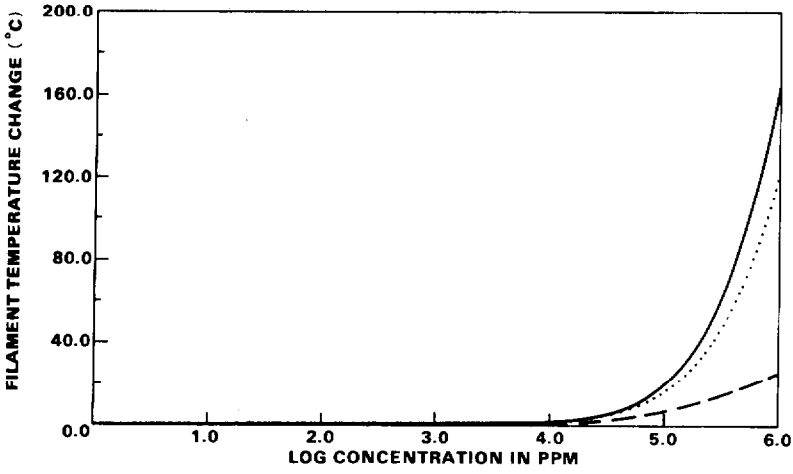

Fig. 9. Effect of sample filament temperature increase. ---, Constant mean temperature; ·····, constant voltage; — —, constant current.

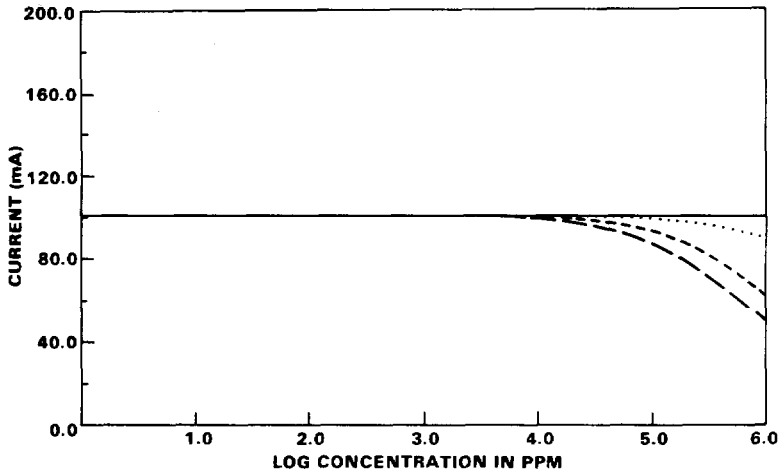

Fig. 10. Sample filament current. ——, Constant current; ···, constant voltage; - - -, constant mean temperature; — — —, constant temperature.

power into the sample filament remains almost constant (Fig. 12), while the dissipation by Q_{cr} increases significantly at higher concentrations owing to the increased temperature of the filament. When the concentration approaches 100%, the dissipation Q_{cr} exceeds that of Q_{con}. In the examples discussed here, this corresponds to a sample filament temperature increase of approximately 120°C.

The coefficient B in eqn. 28 is directly related to the thermal conductivity coefficient for heat transfer through the ends of the filament. In the CV mode the cell used for the measurements became non-linear at a concentration of approximately 26% (non-linear is defined as the concentration at which the sensitivity changes by

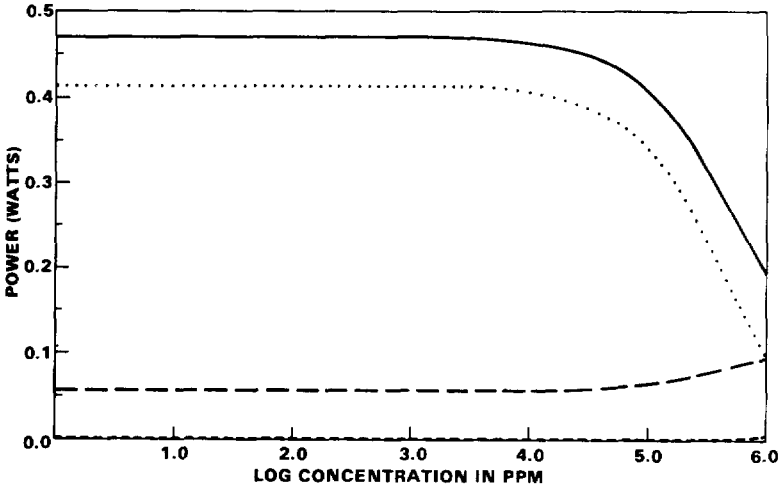

Fig. 11. Power in sample filament (constant mean mode). ——, Power into filament; ···, Q_{con}; — — —, Q_{cr}; - - -, Q_{mt}.

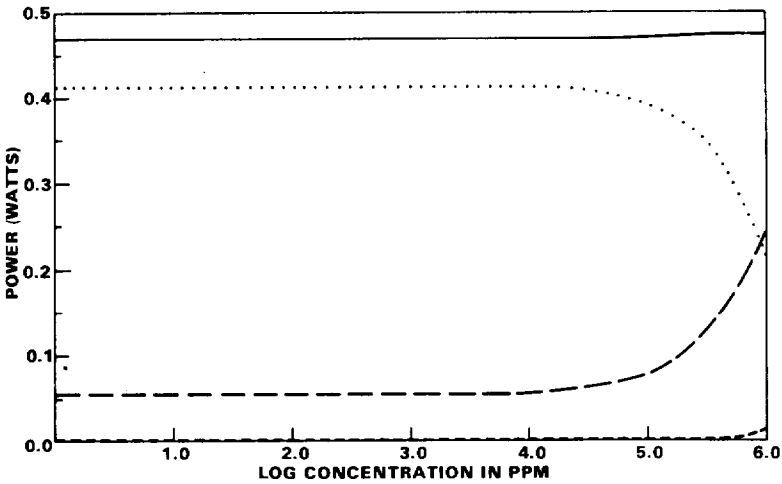

Fig. 12. Power in sample filament (constant voltage mode). ——, Power into filament; ···, Q_{con}; – – –, Q_{cr}; – · –, Q_{mt}.

5%). If the conductivity (B in eqn. 28) could be reduced to half, calculations indicate that the response would be linear to approximately 45% sample concentration at the detector.

CONCLUSION

It has been shown that on the basis of signal-to-noise ratio there is no difference between constant voltage, current or mean temperature modes of operation. The constant temperature mode will usually have a poorer signal-to-noise ratio because of the noise. The data presented here show that the constant voltage mode provides the best linear range. In addition, the decrease in sensitivity at concentrations greater than about 5% can be optimized by a proper choice of heat conduction through the ends of the filament, for any given cell geometry factor G. The improved linear response occurs at the expense of a significant increase in filament temperature at the higher concentrations. When high initial filament temperatures are used, damage may result from accidental air leaks unless some additional mechanism exists to limit the maximum filament temperature.

REFERENCES

1 A. B. Littlewood, *Gas Chromatography*, Academic Press, New York, 1970, Ch. 9.
2 D. J. David, *Gas Chromatographic Detectors*, Wiley, New York, 1974, Ch. 3.
3 A. E. Lawson, Jr., and J. M. Miller, *J. Gas Chromatogr.*, 4 (1966) 273–284.
4 R. T. Wittebrood, *Chromatographia*, 5 (1972) 454–459.
5 P. L. Patterson, R. Commins, U. Christen and K. R. Iwao, *Pittsburg Conference on Analytical Chemistry and Spectroscopy, Cleveland, Ohio, 1976.*
6 H. Kern and M. Elser, *Mikrochim. Acta*, 1 (1978) 319–328.
7 A. L. Lindsay and L. A. Bromley, *Ind. Eng. Chem.*, 42 (1950) 1508.
8 S. Chapman and T. G. Cowling, *The Mathematical Theory of Non-Uniform Gases*, Cambridge University Press, London, 2nd ed., 1961.
9 S. W. Benson, *The Foundations of Chemical Kinetics*, McGraw-Hill, New York, 1960, Ch. 8.